Soft PEG-Hydrogels with Independently Tunable Stiffness and RGDS-Content for Cell Adhesion Studies[a]

Anika M. Jonker, Saskia A. Bode, Addie H. Kusters, Jan C. M. van Hest, Dennis W. P. M. Löwik*

Poly(ethylene)glycol (PEG)-based hydrogels are often used as matrix material for cell culturing. An efficient method to prepare soft PEG gels is by cross-linking via copper-free strain-promoted azide-alkyne cycloaddition (SPAAC). Here, the effect of polymer density and RGDS-content on hydrogel formation and cell adhesion was studied, by varying the total polymer content (10, 20 and 30 mg · mL^{-1}) and the amount of RGDS moieties (0–100%) independently of each other. Rheology studies confirmed the soft nature of the hydrogels ($G' = 25$–$2\,298$ Pa). HOS cells are able to adhere well to all RGDS-containing gels. Interestingly, both HeLa cells and NIH 3T3 fibroblasts showed substantial adherence to 10 and 20 mg · mL^{-1} gels, but with increased hydrogel stiffness (30 mg · mL^{-1}), their cellular adhesion decreased significantly.

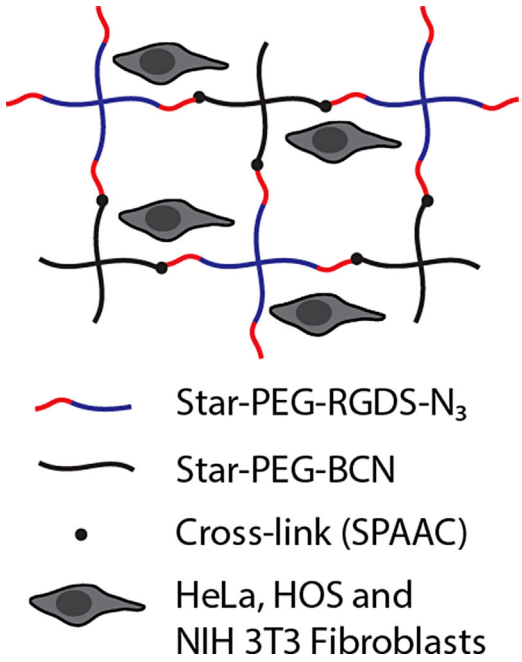

1. Introduction

Hydrogels are water-swollen cross-linked polymeric networks. Due to their high water content, biocompatibility and mechanical properties, hydrogels are promising biomaterials for mimicking the extracellular matrix (ECM).[1–4] Poly(ethylene glycol) (PEG) is a common choice as the polymeric basis for synthetic hydrogels. PEG is hydrophilic, has excellent biocompatibility, low toxicity, and is non-adhesive toward proteins and cells.[5–7] PEG-based hydrogels can be formed by physical or chemical cross-links.[8] Among the chemical cross-linking procedures, the copper-catalyzed "click" reaction between an azide and alkyne (CuAAC) is widely used as it is fast, high-yielding, and modular, but most importantly orthogonal.[9,10] In order to circumvent the necessity of applying cytotoxic copper ions, recently, copper-free strain promoted azide-alkyne cycloaddition (SPAAC),[11–14] thiol-ene chemistry,[15–18] Diels–Alder cycloadditions[19–22] and the SPOCQ reaction (strain-promoted oxidation-controlled cyclooctyne–1,2-quinone cycloaddition) between a catechol and a ring-strained alkyne[23,24] have emerged as efficient alternative cross-

A. M. Jonker, S. A. Bode, A. H. Kusters, Prof. J. C. M. van Hest, Dr. D. W. P. M. Löwik
Radboud University, Heyendaalseweg 135 6525, AJ Nijmegen, the Netherlands
E-mail: d.lowik@science.ru.nl

[a]**Supporting Information** is available online from the Wiley Online Library or from the author.

DOI: 10.1002/mabi.201500110

linking reactions.[25,26] Among others, the SPAAC method has shown its validity in constructing hydrogels which promote cellular adhesion via the incorporation of synthetic adhesion peptides, such as the RGDS sequence.[27–29] DeForest et al.[30] demonstrated that star-shaped PEG functionalized with azide moieties can be clicked to cyclooctyne-containing peptides, leading to hydrogel formation. Also, enzymatically cleavable peptide sequences were efficiently incorporated, making the hydrogels biodegradable.[30] The bio-orthogonal character of these coupling chemistries ensures the functional integrity of the biological motifs in the final hydrogel structure. The broad applicability of these materials was demonstrated by successful cell culturing of a range of cells, such as fibroblasts, human mesenchymal stem cells, and bone marrow derived stromal cells.[30–33]

When culturing cells on hydrogels, it is important to understand how they interact with their surroundings. It has been stated that cells are able to feel the substrate they are attached to and that they will respond based on these external mechanical signals.[34,35] For example, it has been shown that the differentiation of mesenchymal stem cells is dependent on substrate stiffness. Culturing on soft gels (0.1–1 kPa) led to neurons, but myoblasts were formed on stiffer substrates (8–17 kPa) and cells differentiated into osteoblasts on rigid matrices (25–40 kPa).[36] Recent research indicates that these stem cells retain their phenotype on a non-fouling zwitterionic hydrogel, independent of stiffness.[37] In general, most cell lines seem to have a preference to adhere to and grow on stiffer substrates.[35,38–45] However, there remains some debate about the influence of matrix stiffness on cell adhesion, differentiation, and migration. Recently, Trappmann et al.[46] demonstrated that human mesenchymal cells were able to spread and differentiate on collagen-coated polydimethylsiloxane (PDMS) hydrogel surfaces (0.1 kPa–2.3 MPa) independent of their stiffness. Cells on collagen-coated polyacrylamide (PAAm) gels (0.5–740 kPa) on the other hand could only spread on stiff surfaces and differentiated on soft surfaces due to their inability to form focal adhesions. This was confirmed by the fact that decreasing the number of anchoring points on stiff gels resulted in cellular behavior as if there were on soft gels. The authors, therefore, stated that cells apply a mechanical force on substrate-bound ECM and need the feedback to make cell-fate decisions. These results, thus, show that it is not the stiffness, but the mechanical feedback of the ECM that influences cell behavior.[46] On the other hand, Missirlis and Spatz[47] studied the effect of substrate elasticity on fibroblast adhesion using PEG hydrogels (5.5–65 kPa). They found that cells respond to differences in substrate elasticity and were unlikely to respond to differences in ligand tethering. Fibroblasts were found to spread increasingly better on stiffer substrates. These results, thereby, support the general idea that most cells prefer stiffer substrates.[47] However, there are also studies that reported different cellular responses to hydrogel stiffness. Caruso et al. revealed that HeLa cell adhesion on soft poly (methacrylic acid) PMA_{SH} hydrogels (2.5 kPa) decreased with increasing film stiffness. They found negligible differences in the hydrogel film roughness, hydrophobicity, and charge and stated that the differences in cell adhesion are caused by the mechanical properties of the gel.[48] Robinson et al. found that proliferation of NIH 3T3 cells and HUVECs was larger on gels with a lower strength. On the other hand, human vascular smooth muscle cells and adventitial fibroblasts showed enhanced growth on stiffer surfaces.[49] All together, these examples highlight the need to further study the influence of the synthetic matrix on cellular adhesion, migration and differentiation.[3]

So far, most cellular adhesion studies have been performed with stiff substrates, usually exceeding the stiffness range of most mammalian organs, which have elastic moduli (G′) between 100 and 10 000 Pa.[43,44,46,47,50] In this study, we aim to investigate how different cell lines respond to various soft hydrogels. For this purpose, we fabricated soft hydrogels with PEG as the polymeric basis, using bicyclo[6.1.0]nonyne (BCN) based copper-free click chemistry.[13] In order to promote cellular adhesion of our PEG hydrogels, an RGDS peptide motif was incorporated in the polymeric network (Figure 1). These clickable hydrogels constitute a platform that allows us to vary both the RGDS content and the polymer density independently of each other. In this way, we intend to get insight on the influence of the stiffness of soft hydrogels in combination with the amount of adhesion motifs on the cell viability of three different cell types.

2. Experimental Section

Polymers were synthesized, as described below, and were characterized with ^{1}H-NMR and MALDI-TOF analysis (see Supporting Information). Materials and methods, further synthesis protocols, peptide synthesis, IR spectroscopy, additional rheology data, confocal microscopy images, and *p*-values can be found in the Supporting Information.

2.1. Star-PEG-BCN

To a dry reaction flask was added 4-armed 10 kDa poly(ethylene glycol)-NH_2 HCl salt (600 mg, 0.06 mmol), (1*R*,8*S*,9*S*)-bicyclo[6.1.0] non-4-yn-9-ylmethyl succinimidyl carbonate (BCN-OSu; 87.4 mg, 0.30 mmol), and 100 μL triethylamine (100 μL, 0.72 mmol) in dry DCM (25 mL). The reaction mixture was stirred at r.t. overnight under N_2 atmosphere. Extraction was performed with 2M NaOH (3×25 mL). The organic layer was dried over $MgSO_4$ and concentrated in vacuo. The residue was purified by column chromatography on silica gel (MeOH:DCM 2:98, followed by

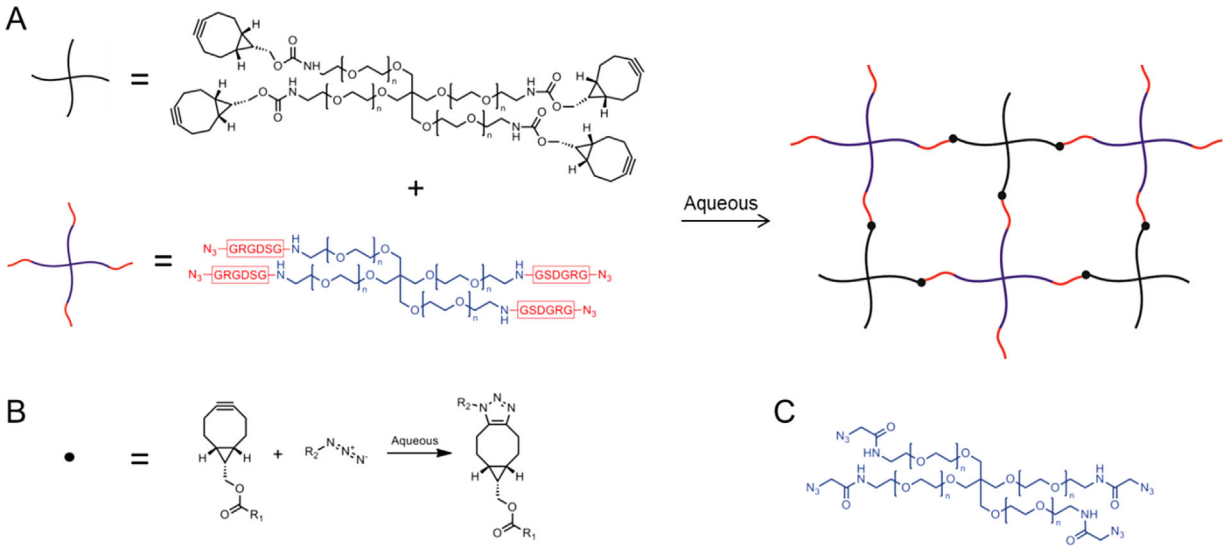

Figure 1. Hydrogel formation. (A) Mixing of star-PEG-BCN with star-PEG-RGDS-N_3 yields a stable hydrogel network (containing 100% RGDS). (B) Cross-links are formed by copper-free click chemistry. (C) The composition of the hydrogel network can be adjusted by mixing in certain amounts of star-PEG-N_3, and thereby changing the total RGDS content. Furthermore, the RGDS-polymer can also be replaced by a RDGS-containing star-PEG (star-PEG-scrambled (structure not shown).

10:90). The product was afforded as a white powder after freeze-drying from dioxane (406 mg, 63%).

2.2. Star-PEG-N_3

To 4-armed poly(ethylene glycol)-NH_2 HCl salt (800 mg, 80 μmol) in DCM (25 mL) was added subsequently benzotriazol-1-yl-oxy-tris dimethylaminophosphonium hexafluorophosphate (BOP; 283 mg, 0.64 mmol), azido acetic acid (65 mg, 0.64 mmol) and D*i*PEA (328 μL 1.92 mmol). The reaction mixture was stirred overnight at r.t and extracted with 1 M $KHSO_4$ (5 × 50 mL) and brine (1 × 50 mL). The organic layer was dried over $MgSO_4$ and concentrated in vacuo. The compound was purified by column chromatography on basic aluminum oxide, using MeOH:DCM (10:90) as eluent. Freeze-drying from dioxane afforded the product as a white powder (760 mg, 92%).

2.3. Star-PEG-RGDS-N_3 and Star-PEG-Scrambled

To star-poly(ethylene glycol)-NH_2 HCl salt (750 mg, 75 μmol) in DCM (20 mL) was added subsequently BOP (199 mg, 0.45 mmol), protected peptide (azidoGly-Arg-Gly-Asp-Ser-Gly-OH or azidoGly-Arg-Asp-Gly-Ser-Gly-OH, 422 mg, 0.45 mmol), and D*i*PEA (314 μL, 1.8 mmol). The reaction mixture was stirred overnight at r.t. Extraction was performed with 1 M $KHSO_4$ (4 × 60 mL) and brine (1 × 60 mL), after which the organic layer was dried over $MgSO_4$. Column chromatography on basic aluminum oxide (MeOH:DCM; 10:90) afforded white powders after freeze-drying from dioxane (RGDS: 885 mg, 86%; scrambled: 896 mg, 87%).

The protected peptide-star-PEG construct (350 mg; 25.6 μmol) was treated with TFA:TIS:H_2O (95:2.5:2.5; 8 mL) for 4 h at r.t. The reaction mixture was concentrated and co-evaporated with toluene (4 × 30 mL). The product was dissolved in water and dialyzed against 800 mL water using dialysis membranes with a MW cut-off of 3 500 Da. Dialysis was performed for 5 d under regular exchange of the water (twice a day). After dialysis, the products were obtained as white solids by freeze-drying (RGDS: 289 mg, 92%; scrambled: 298 mg, 95%).

2.4. Hydrogel Formation

Hydrogels were prepared by weighing off equal amounts of star-PEG-BCN and star-PEG-N_3 with a total polymer concentration of 10, 20, or 30 mg · mL^{-1}. For example, a typical 30 mg · mL^{-1} PEG hydrogel was obtained by dissolving 3.00 mg star-PEG-BCN in 100 μL MilliQ. To this solution was added 100 μL star-PEG-N_3 (30 mg · mL^{-1}, in MilliQ). The two hydrogel components were mixed by vortexing and left at room temperature to allow gel formation. For a peptide-containing hydrogel, stock solutions of star-PEG-N_3 and star-PEG-RGDS/star-PEG-RDGS were added to star-PEG-BCN. For example, a 50% RGDS-containing gel (20 mg · mL^{-1}) was prepared by adding 50 μL star-PEG-N_3 and 50 μL star-PEG-RGDS (each 20 mg · mL^{-1} in MilliQ) to a star-PEG-BCN solution (2 mg in 100 μL MilliQ).

2.5. Rheology

The storage (G′) and loss modulus (G″) of the hydrogels were measured using an AR2000ex rheometer (TA instruments). All measurements were performed using a flat steel plate geometry (20 mm, gap size 500 μm) and were performed at a temperature of 20 °C. Hydrogel solutions were prepared at different polymer concentrations and RGDS-content. A molar ratio of 1:1 between the alkyne and azide groups was used to ensure complete cross-linking.

Hydrogel solutions were loaded on the rheometer as liquid (200 μL) and were measured during the gelation process. To minimize evaporation, a solvent trap was utilized which was filled with water. Initially, a strain sweep measurement was conducted on cured gels to determine the linear viscoelastic range, by measuring between 0.1 and 1 000% strain at an angular frequency of 10 rad · s^{-1}. Within this range, a strain percentage (1%) was chosen to perform further measurements. Oscillatory time sweep measurements were measured at a constant strain of 1% and an angular frequency of 10 rad · s^{-1} and were continued until stable values of G′ were obtained. Typically, time sweep tests were conducted for 2.5 h (30 mg · mL^{-1}), 5.5 h (20 mg · mL^{-1}) and 16 h (10 mg · mL^{-1}). Additionally, overnight time sweep measurements (16 h) were performed for 30 mg · mL^{-1} hydrogels containing 0% peptide, 100% RGDS, and 100% scrambled peptide (Table S1, $n = 2$). All other rheology measurements were performed with $n = 3$ or $n = 4$.

2.6. Swelling

Hydrogels (250 μL) were prepared from star-PEG-BCN and star-PEG-N_3 following the general protocol using total polymer concentrations of 10, 20, and 30 mg · mL^{-1}. Gels were allowed to cross-link overnight, after which they were weighed to obtain the mass after gelation (Mg). After swelling for 24 h in MilliQ water, gels were weighed again, yielding the mass after swelling (Ms). The swelling ratio was given as $Q = Ms/Mg$. Samples were made with $n = 5$ for each polymer concentration (Table S2).

2.7. WST-8 Assay

Hydrogels were formed in a 96-well plate; to each well 75 μL hydrogel solution (see hydrogel formation) was added. The plate was wrapped with parafilm and gels were allowed to form overnight (24 h). All samples were measured in triplo. As a positive control, a number of wells were coated with 1% gelatin to obtain 100% viable cells. NIH 3T3 fibroblasts were plated at a density of 18 000 cells in 100 μL per hydrogel-containing well. Cells cultured on the hydrogels were incubated for 18 h (37 °C, 7.5% CO_2). Cells were examined under a standard inverted microscopy (Olympus CK2) prior to WST-8 addition, to evaluate the total cell count visually. Media were replaced by 100 μL WST-8 (1:10 in DMEM) and incubation was performed for 4–6 h. The absorbance of the WST-8 solution was measured at 450 nm using a Tecan Infinite M200 Pro plate reader. For all samples and the gelatin control, the background absorbance was subtracted, which was the absorbance measured in wells that only contained the WST-8 dye in medium. Total cell count for all hydrogels was calculated as a percentage of the positive gelatin control, which was set to 100% viable cells.

2.8. Confocal Microscopy

Hydrogel solutions were prepared, following the general protocol of hydrogel formation. All RGDS-hydrogels contained 50% of the cell adhesion domain. An 8-chambered coverslip (Nunc, Wiesbaden, Germany) was coated with gel by addition of a small layer of hydrogel solution. The coverslip was wrapped with parafilm and gels were allowed to cure for 24 h at r.t. In each well, 40 000 cells in 250 μL medium were seeded. Wells coated with gelatin were used as positive control. Cells were incubated overnight (37 °C, 7.5% CO_2). After this incubation period, the cells were treated with the live/dead staining, which was prepared by diluting calcein-AM and ethidium homodimer-1 (EthD-1) in PBS to obtain a concentration of 4 mM calcein-AM and 8 mM EthD-1 for HeLa and HOS cells, the concentration was lowered to 1.33 mM calcein-AM and 2.67 mM EthD-1 for NIH 3T3 fibroblasts. The samples were allowed to rest for 10 min, after which they were immediately analyzed by confocal laser scanning microscopy. Calcein was excited with the 488 nm line of an argon ion laser, and emission was collected between 494 and 515 nm. EthD-1 was excited with the 561 nm line of a yellow diode laser and emission was collected between 600 and 625 nm. Using the ImageJ software, overlay images of the calcein and EthD-1 signals were produced (Figure S10–S12).

3. Results and Discussion

3.1. Hydrogel Design

Hydrogels were fabricated using 4-armed poly(ethylene glycol) ($M_n = 10$ kDa, star-PEG) as the polymeric basis. As cross-linking methodology, we used copper-free strain-promoted click (SPAAC) chemistry, with a bicyclo[6.1.0] nonyne (BCN) derivative as the ring-strained alkyne.[13] Star-PEG-amine was functionalized with either an azide or BCN moiety, by coupling of azido acetic acid and BCN-OSu, respectively (Figure 1). Additionally, we also synthesized the corresponding di-functionalized PEG analogues. Hydrogels were formed by combining equimolar amounts of star-PEG-BCN and star-PEG-N_3, or by replacing one of the star-polymer components by di-functionalized PEG. Upon mixing the components in water, the click reaction commenced, leading to the formation of a polymeric network. Cross-linking took place without the need of additional chemicals or further processing. Gel formation was qualitatively examined via the inverted vial test. We investigated the minimal polymer concentration required for gelation to occur, by varying the total polymer content from 5 up to 30 mg · mL^{-1}. Very soft hydrogels were formed overnight for the combination of star-PEG-BCN with star-PEG-N_3 at a total polymer concentration of 10 mg · mL^{-1} (1 wt%). This appeared to be the minimum gelation concentration, since only viscous solutions were obtained at 5 mg · mL^{-1}. Increasing polymer concentration resulted in faster gelation times. Hydrogels could also be obtained when combining star-PEG polymers with di-functionalized PEG, but gelation times were significantly longer. When star-shaped polymers are used for gelation, more branching points are available, so a denser network is formed, leading to faster gelation. We therefore decided to continue with the star-shaped polymers for further studies.

Next, IR-spectroscopy was performed on 30 mg · mL^{-1} gels to confirm that gelation concurred via the click

reaction. When equimolar amounts of azide and BCN were used, the typical azide-signal around 2 100 $\cdot$ cm^{-1} could not be detected after hydrogel formation, while it was clearly present before cross-linking. When an excess of star-PEG-N_3 was utilized, the azide-signal did not fully disappear after gelation had occurred (Figure S7).

Now that we confirmed that copper-free azide-BCN cycloaddition chemistry is suitable as a cross-linking method for soft hydrogel formation, we aimed to introduce peptide functionalities in the PEG polymer network (Figure 1). To be able to investigate the cellular adhesion properties of the hydrogels, we incorporated the well-known RGDS adhesion domain.[27–29] First, this peptide was synthesized using standard Fmoc solid phase peptide synthesis, with coupling of azido-acetic acid as the final residue. The employed Barlos solid phase resin allowed mild resin cleavage to keep all acid-labile side-chain protecting groups in place. Coupling of the peptide to star-PEG-NH_2 could therefore be performed selectively at the C-terminus. This method allowed us to easily obtain azidoGly-Arg-Gly-Asp-Ser-Gly functionalized star-PEG, which is further referred to as star-PEG-RGDS-N_3 (Scheme 1). We also synthesized the scrambled peptide (azidoGly-Arg-Asp-Gly-Ser-Gly) polymer construct star-PEG-scrambled, which was not expected to be able to induce cell adhesion. With these building blocks in hand, we were able to fabricate various soft hydrogels. Our modular approach allows us to vary both the polymer density and RGDS-content independently of each other. We could adjust the polymer density by varying the total polymer content. Hydrogels were prepared in the concentration range 10–30 mg $\cdot$ mL^{-1}. Furthermore, we tuned the RGDS content by mixing in both star-PEG-RGDS-N_3 and star-PEG-N_3, for cross-linking to star-PEG-BCN.

3.2. Rheology

The mechanical properties of the PEG- and PEG-RGDS-hydrogels were determined using rheology. The storage (G′) and loss modulus (G″) were measured using an oscillatory time sweep test. Hydrogels were prepared with varying total polymer concentration (10–30 mg $\cdot$ mL^{-1}) using a molar ratio of 1:1 between the azide and alkyne groups. The cross-over point at which G′ exceeds G″ was determined as an estimate of the point of gelation. With increasing polymer concentration, the time to reach this point of gelation decreased. Gel formation started after 22 min for the 30 mg $\cdot$ mL^{-1} PEG-only hydrogel, where the gelation time increased to 47 min for 20 mg $\cdot$ mL^{-1} and 338 min for 10 mg $\cdot$ mL^{-1} (Table 2). After reaching the cross-over point, G′ steadily increased for all hydrogels and reached a final value which was much larger than G″ (Figure 2). Typically, G″ values in the background range were obtained (0 $\pm$ 5 Pa). A significant increase in final G′ was found after set time points with increasing polymer content. Hydrogels of 10 mg $\cdot$ mL^{-1} showed a G′ of 25 Pa (16 h), while values for 20 mg $\cdot$ mL^{-1} and 30 mg $\cdot$ mL^{-1} were 1 192 Pa (5.5 h) and 2 298 Pa (2.5 h), respectively (Table 1). Frequency sweep measurements were conducted on all cured hydrogels and G′ and G″ were found to be independent of frequency. This corresponds to a predominantly elastic composition of the PEG gels (Figure 2). These results indicate that the PEG materials show typical hydrogel behavior (G′ >> G″); the obtained hydrogels are highly elastic and, as expected, stronger gels are obtained with increasing polymer content.[51] Importantly, as intended, we obtained PEG hydrogels with relatively low stiffness. Our hydrogels have elastic moduli in the soft tissue range, comparable to that of most mammalian organs (G′ = 100–10 000 Pa) and are softer than most materials reported thus far.[50] Swelling ratios of the 10, 20, and 30 mg $\cdot$ mL^{-1} hydrogels were determined to be 1.032 $\pm$ 0.004, 1.008 $\pm$ 0.004, and 1.013 $\pm$ 0.011, respectively. Due to the low polymer content (1–3 wt %), these gels have a high water content, resulting in hardly any swelling. The polymer density of the hydrogels can thus only be varied effectively by appyling different conentrations of star-PEG polymers during hydrogel preparation. Next, we studied the mechanical properties of RGDS-containing hydrogels. We measured hydrogels containing 50 and 100% RGDS for all three polymer concentrations. Lower G′ values were obtained than for PEG-only hydrogels after set time points (Table 1). Since the cross-over point was observed at a later time-point (Table 2), we estimated that gelation was likely to occur more slowly in RGDS-containing hydrogels. To rule out the possibility that this pattern is sequence dependent, we also tested hydrogels containing the scrambled peptide sequence and found the same effect (G′ = 1 355 Pa $\pm$ 65, 100% scrambled, 30 mg $\cdot$ mL^{-1}) (Figure S9). To test our hypothesis that gelation occurs slower with peptide-containing hydrogels,

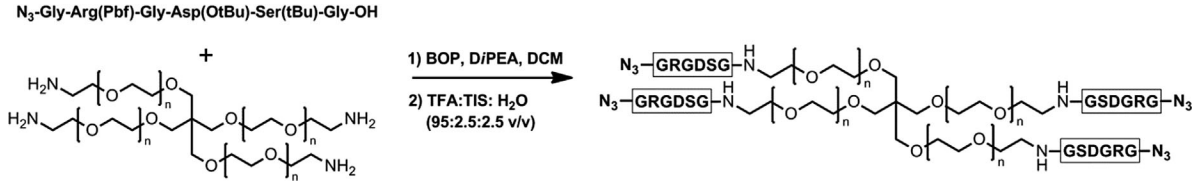

Scheme 1. Synthesis of star-PEG-RGDS-N_3.

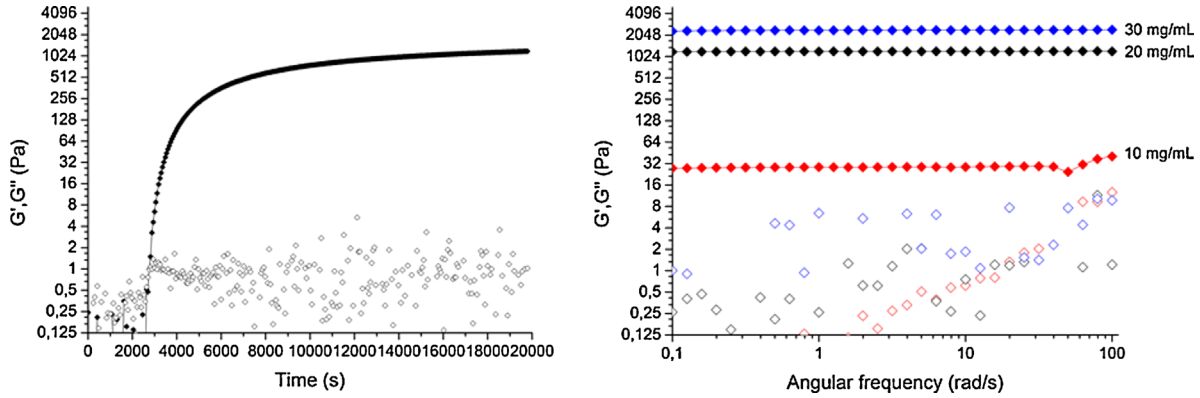

Figure 2. Rheology data of the PEG-hydrogels, G′ is represented by closed symbols, G″ by open symbols. Left: time sweep measurement of the 20 mg · mL^{-1} PEG-hydrogel. After reaching the gelation point (47 min), G′ steadily increases and reaches a final value (1 192 Pa) which is much larger than G″. Right: frequency sweep measurements of the 10, 20, and 30 mg · mL^{-1}, showing that hydrogels have a predominantly elastic composition.

we measured the 30 mg · mL^{-1} hydrogels overnight (16h). We measured star-PEG, star-PEG-RGDS-N_3 (100%) and star-PEG-scrambled (100%) and found G′ values of 3 186 Pa, 2 863 Pa and 3 086 Pa, respectively (Table S1). Comparable G′ values were obtained with or without peptide for fully cured gels. We can therefore conclude that incorporation of peptide sequences does not hinder network formation, and thus, albeit slower, yields stable hydrogels.

3.3. Cell adhesion Studies

After synthesizing and studying the mechanical properties of our RGDS-containing PEG-based gels, we set out to investigate the cell adhesion properties of these soft hydrogels. Since our hydrogel formation method easily allows us to vary the amount of RGDS present in the network, an RGDS concentration range was studied. We prepared hydrogels in the three polymer concentrations (10, 20, and 30 mg · mL^{-1}) containing 1, 5, 10, 25, 50, 75, and 100% RGDS, in order to investigate how much RGDS is required to give cellular adhesion. This corresponds to a concentration range of RGDS clusters from 5 μM (1% RGDS, 10 mg · mL^{-1}) up to 1 500 μM (100% RGDS, 30 mg · mL^{-1}). If we assume that clusters of four peptides are homogeneously distributed throughout the polymeric network, and that cells are able to interact with these peptides within 5 nm from the surface, we can calculate the amount of RGDS clusters in the top surface layer of the hydrogels.[47,52] We calculated this range to be between 15 and 4 500 RGDS clusters · μm^{-2}. Massia and Hubbell demonstrated that a peptide spacing of 140 nm is sufficient for focal contact formation, which corresponds to 60 peptides · μm^{-2}.[53] In the weakest hydrogel (10 mg · mL^{-1}) with 1% RGDS (15 clusters · μm^{-2}), the adhesion points might thus be too far from each other for decent cellular adhesion, although each cluster already contains 4 RGDS moieties. Apart from the lowest RGDS concentrations, the range used here corresponds to previous studies on cell adhesion.[47,54]

To investigate the influence of RGDS-content on cell adhesion, gels with an RGDS concentration range (1, 5, 10, 25, 50, 75, and 100%) were tested in a WST-8 assay to measure the number of viable cells. Upon cellular reduction,

Table 1. Hydrogel strength G′ (Pa) measured by rheology. Values were recorded after set time points of 16, 5.5, and 2.5 h for 10, 20 and 30 mg · mL^{-1}, respectively. All measurements performed with $n = 3$ or $n = 4$. Hydrogel strength increases with increasing polymer density. Incorporation of the RGDS-peptide results in lower moduli.

RGDS	G′ 10 mg · mL^{-1}	G′ 20 mg · mL^{-1}	G′ 30 mg · mL^{-1}
0%	25 ± 3	1192 ± 23	2 298 ± 67
50%	18 ± 16	841 ± 21	2 094 ± 64
100%	12 ± 1	611 ± 56	1 496 ± 77

Table 2. Cross-over points (G′ exceeds G″) in minutes for 10, 20, and 30 mg · mL^{-1} hydrogels containing 0, 50, and 100% RGDS. Gelation time increases with incorporation of the peptide moiety. * = Single measurement, the other 10 mg · mL^{-1} gels were not constantly measured during the gelation process.

RGDS	Gelation point 10 mg · mL^{-1} [min]	Gelation point 20 mg · mL^{-1} [min]	Gelation point 30 mg · mL^{-1} [min]
0%	338 ± 25	47 ± 2	22 ± 1
50%	423*	53 ± 1	25 ± 2
100%	478*	63 ± 2	29 ± 1

the cell-permeable WST-8 is converted into the water soluble formazan, of which the absorbance can be measured.[55] As a negative control, PEG-only hydrogels were tested. Since PEG is known to be non-adhesive, cellular adherence to these hydrogels is unlikely to occur.[5–7] As a second negative control we also tested the star-PEG-scrambled (RDGS) hydrogels. Based on the rheology studies, we left the gels overnight to allow them to fully cure. The next day, NIH 3T3 fibroblasts were seeded on each hydrogel. Gelatin-coated wells were used as positive control; the total number of viable cells in these wells was set to 100%. The total cell count of the hydrogel samples was calculated as a percentage of the gelatin control. The WST-8 assay performed with the RGDS concentration range revealed that changing the RGDS content did not have an influence on the total amount of viable cells (Figure 3). Within one hydrogel stiffness similar viability percentages were obtained for all different RGDS concentrations. Interestingly, clear differences in total cell count were observed between gels with varying stiffness (10, 20, and 30 mg · mL^{-1}). The amount of viable cells on the 10 and 20 mg · mL^{-1} resembled the gelatin control, but their number clearly decreased on the 30 mg · mL^{-1} gels (Figure 3). Since the amount of RGDS did not show to have an influence on the total cell count, we decided to only study the influence of hydrogel stiffness on cell adhesion in further experiments.

Apart from the NIH 3T3 fibroblasts, we chose to study HeLa and human osteosarcoma (HOS) cells. We were interested in these cell lines, since they originate from different tissue. HOS cells originate from human bone tumor and might be more likely to adhere to stiffer surfaces. HeLa cells and NIH 3T3 fibroblasts are both derived from softer tissues, and are therefore interesting to compare to HOS cells. We studied the hydrogels with confocal laser scanning microscopy (CLSM) using a live/dead assay to assess viability. This assay consists of two dyes, one to color living cells (calcein-AM) and one for dead cells (ethidium homodimer-1, EthD-1). Calcein-AM is cell-permeable and is converted to the green fluorescent calcein by intracellular esterase activity of live cells. Ethidium homodimer-1 can only enter cells with a damaged membrane, and then binds to nucleic acids, leading to a bright red fluorescence. We first investigated whether cell adhesion is specific for the RGDS sequence by performing the live/dead assay with HeLa cells seeded on 20 mg · mL^{-1} PEG-only, RGDS-containing, and scrambled hydrogels (Figure 4). Since we found that varying the RGDS content does not have an influence, we decided to perform further studies with gels containing 50% RGDS. The live/dead assay showed red fluorescent cells for PEG-only and scrambled hydrogels, showing that cells do not remain viable. Furthermore, their transmission images revealed that these cells have a round morphology. As expected, gels lacking a cell adhesion motif are not suitable substrates for cellular adherence (SI, Figure S13). Incorporation of the RGDS-motif turned the hydrogels into an appropriate substrate for cellular adhesion, as seen by the large number of green fluorescent cells and their spread morphology (Figure 4).

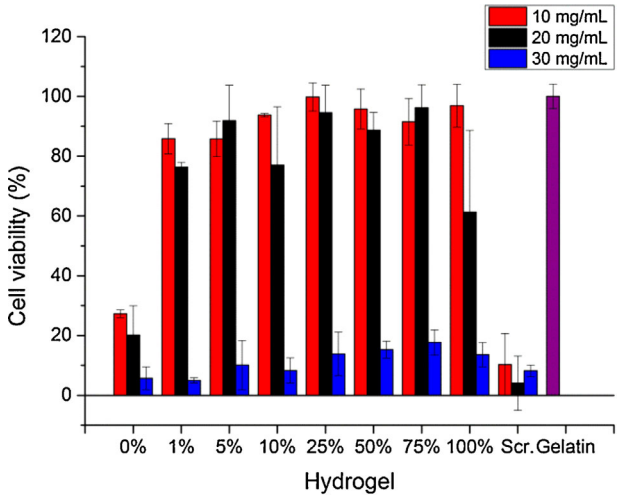

Figure 3. WST-8 assay with NIH 3T3 fibroblasts, the *x*-axis shows the different hydrogel compositions, the *y*-axis shows the cell viability calculated based on the positive gelatin control (set to 100%). Varying of the RGDS content does not have an influence on total cell count. The 10 and 20 mg · mL^{-1} hydrogels have a high cell count, in contrast to the stiffest hydrogel of 30 mg · mL^{-1} which shows a remarkable decrease in the total amount of living cells.

Next, the live/dead assay was performed on the RGDS-containing hydrogels with the three cell types (HeLa, NIH 3T3, and HOS) (Figure 5, Figure S10–S12). All hydrogel coatings were prepared in the same manner, containing 50% RGDS. Hydrogels only differed in the total polymer content (10, 20, 30 mg · mL^{-1}) and thus in gel stiffness. Many live cells with a spread morphology were observed for HOS cells on all hydrogels, indicating that these bone marrow-derived cells were able to spread on RGDS-hydrogels, independent of their stiffness (Figure 5 and **6**, Figure S12). The live/dead assay performed with HeLa cells and NIH 3T3 fibroblasts revealed many live cells for the 10 and 20 mg · mL^{-1} hydrogels, which nicely adhered in a spread morphology. Interestingly, cell adherence on the stiffest hydrogel (30 mg · mL^{-1}) was clearly diminished for both HeLa cells and NIH 3T3 fibroblasts. The assay revealed a lower amount of adhered cells in both samples; however these cells were still viable as seen by the green fluorescent signals. NIH 3T3 fibroblasts on the 30 mg · mL^{-1} gel showed a mixture of cells with a spread and round morphology, whereas HeLa cells mainly had a round morphology. Differences in cell adhesion between 10 or 20 mg · mL^{-1} and 30 mg · mL^{-1} were significant, as determined by counting

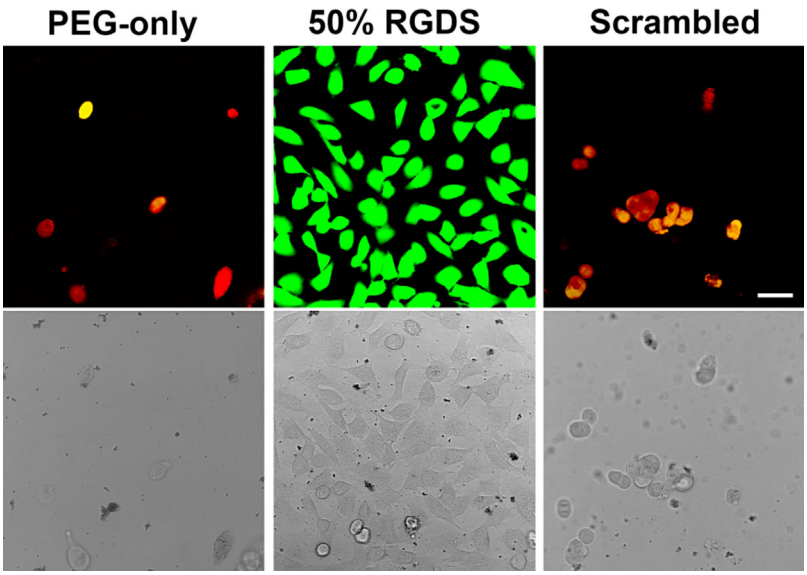

Figure 4. Cell viability images for the live/dead assay on 20 mg · mL^{-1} hydrogels. Images are composed from overlays of the calcein-AM (green) and ethidium homodimer-1 (EthD-1, red) channels. Dead cells (red) were observed on PEG-only (left) and scrambled hydrogels (right), live cells (green) were found on RGDS-containing hydrogels (center). Cell spreading is thus specific for the RGDS sequence. Upper picture: confocal fluorescence, lower picture: transmission image. Scale bar represents 50 μm for all micrographs.

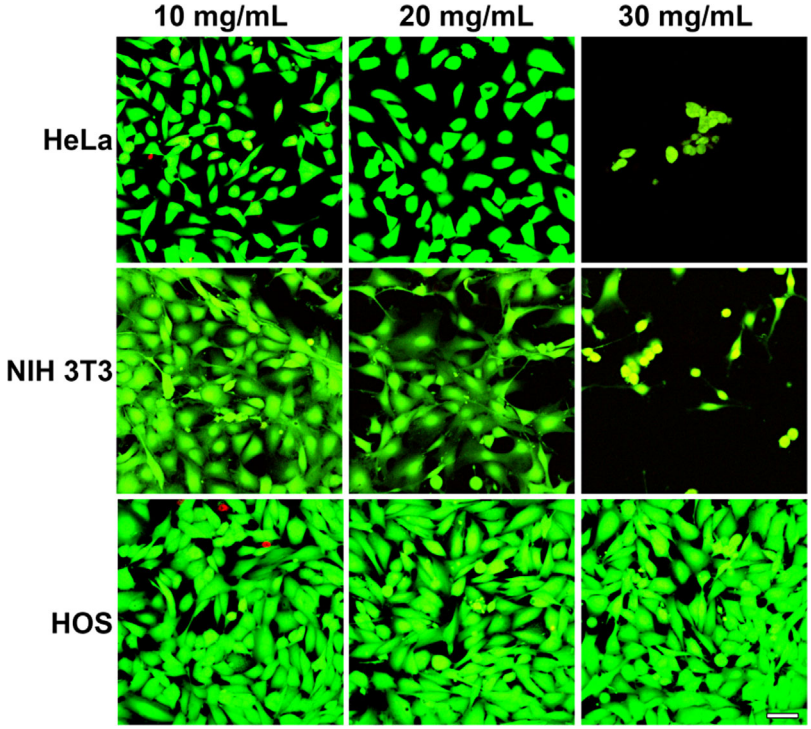

Figure 5. Representative confocal fluorescence micrographs for HeLa, NIH 3T3 fibroblasts and HOS cells seeded on RGDS-containing hydrogels with different polymer densities. Cells are stained with calcein (green) and EthD-1 (red). Pictures are obtained from overlay images of the calcein and EthD-1 channels. From left to right: 10, 20, and 30 mg · mL^{-1} hydrogels, all containing 50% RGDS. Scale bar corresponds to 50 μm for all micrographs (for cell count, see Figure 6) (for transmission images, see Figure S10–S12).

the total number of adhered cells (Figure 6, Table S3). Both HeLa cells and NIH3T3 fibroblasts are derived from softer tissues than HOS cells and experience difficulties with adherence to the stiffest hydrogel (30 mg · mL^{-1}) (Figure 5 and 6; Figure S10 and S11).

3.4. Discussion

The live/dead assay revealed that 10 and 20 mg · mL^{-1} RGDS-containing hydrogels are suitable substrates for cell adhesion for all cell-types tested. Many live HOS cells with a spread morphology were also found for the stiffest hydrogel of 30 mg · mL^{-1}, in contrast to the results for HeLa cells and NIH 3T3 fibroblasts for which the amount of spread cells was clearly decreased. Because we found that the RGDS concentration does not have an influence, the only difference with the 30 mg · mL^{-1} hydrogels is the increased total polymer concentration, which affects the mechanical properties of the gel. Swelling of the gels was not taken into account, since none of the gels absorbed water due to their high water content. Based on literature results, we assume that the surface chemistry of the hydrogels is not affected by the increased polymer density.[41,48] Hence, the increased stiffness is likely to be the reason for the decreased cellular adhesion properties of the 30 mg · mL^{-1} hydrogels. These results are in contrast to the general consensus from literature that most cells seem to have a preference for stiffer substrates. There is, however, still debate on the influence of the mechanical properties on cellular adhesion. Several studies indicate that stiffness is an important factor to determine cell adhesion, whereas others state that it is the mechanical feedback of the ECM.[35,38–47,50] Important to note in this discussion is that most hydrogels studied thus far have elastic moduli (G′) in the order of magnitude of kPa, or even MPa. The high stiffness of these gels might also influence the adhesion behavior of cells. Caruso et al. investigated this effect by developing soft PMA_{SH} hydrogel films with a strength up to 2 500 Pa, thus in the

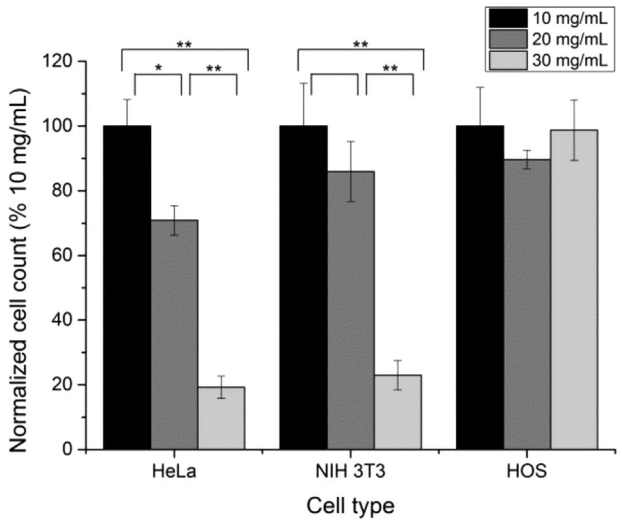

Figure 6. Cell count, based on live-dead assay confocal images ($n = 3$, Figure 5). The amount of counted cells on 10 mg · mL^{-1} hydrogels was set to 100%. HeLa and NIH 3T3 showed significant differences in the number of cells adhered to 10 or 20 mg · mL^{-1} and the amount on 30 mg · mL^{-1} gels. HOS cells did not show significant differences with varying hydrogel stiffness (for *p*-values, see Table S3).

same range as our PEG-hydrogels.[48] They found the same pattern as we did and thus opposite to what others have reported; decreasing cell adhesion was observed with increasing hydrogel stiffness. Negligible differences were seen in the surface chemistry of hydrogel films with various strengths, showing that cells respond to substrate elasticity. The authors postulated that this effect was due to the enhanced cell-film contact area for softer hydrogels. Additionally, the Heilshorn group studied spreading of fibroblasts on soft ELP-PEG gels. Many fibroblasts (≈60%) spread on gels with a modulus of 1 300 Pa, whereas only 3% of the cells showed a spread morphology on the stiffer hydrogel (2 500 Pa).[56] Moreover, the same effect was found by the Anseth group for human mesenschymal stem cells adhered to thiol-ene photopolymerized PEG-gels. Gels with a low G′ modulus (110 Pa) showed greater cell spreading than stiffer gels (1 180 Pa).[57] Results from the Caruso, Heilshorn and Anseth group are thus in good agreement with our data using SPAAC cross-linked PEG-hydrogels and were all performed on soft hydrogels (up to 2 500 Pa).[48,56,57] Taken together, this indicates that stiffness seems to have an influence on the cellular adhesion of *soft hydrogels* and results in decreased cellular adhesion with increasing hydrogel stiffness.

4. Conclusion

We used bio-orthogonal copper-free azide-BCN cycloaddition chemistry (SPAAC) for the construction of soft PEG-based hydrogels. Hydrogels with different polymer densities were obtained by varying the total polymer content. From rheology studies to determine stiffness, storage moduli (G′) in the range of 25 Pa (10 mg · mL^{-1}) till 2 298 Pa (30 mg · mL^{-1}) were obtained. The cellular adhesion motif RGDS could easily be incorporated in the hydrogel network. Gels containing the peptide moiety formed slower, but still yielded stable networks. The RGDS content and polymer density could be varied independently of each other. Live/dead assay studies revealed that HOS cells are viable and well-spread on all RGDS-containing hydrogels, independent of their stiffness. For both HeLa cells and NIH 3T3 fibroblasts many live cells were found on the 10 mg · mL^{-1} (25 Pa) and 20 mg · mL^{-1} (1 192 Pa) gels. With increased hydrogel stiffness (30 mg · mL^{-1}, 2 298 Pa), cellular adhesion decreased. For hydrogels in the very soft regime we studied, hydrogel stiffness seems to be a determining factor in cellular adhesion of HeLa cells and NIH 3T3 fibroblasts.

Acknowledgements: The authors would like to thank Sander Leeuwenburgh for fruitful discussions. The department of General Instruments of the Radboud University Nijmegen is acknowledged for providing light microscopy services. This work was financially supported by the Dutch Science Foundation (NWO, VICI), by the Ministry of Education, Culture and Science (Gravitation program 024.001.035) and by the IOP Self-Healing Materials program.

Received: March 27, 2015; Revised: May 20, 2015; Published online: June 11, 2015; DOI: 10.1002/mabi.201500110

Keywords: cell adhesion; SPAAC; stiffness; hydrogel

[1] S. Van Vlierberghe, P. Dubruel, E. Schacht, *Biomacromolecules* **2011**, *12*, 1387.
[2] N. A. Peppas, J. Z. Hilt, A. Khademhosseini, R. Langer, *Adv. Mater.* **2006**, *18*, 1345.
[3] P. M. Kharkar, K. L. Kiick, A. M. Kloxin, *Chem. Soc. Rev.* **2013**, *42*, 7335.
[4] A. M. Jonker, D. W. P. M. Löwik, J. C. M. van Hest, *Chem. Mater.* **2012**, *24*, 759.
[5] J. Zhu, *Biomaterials* **2010**, *31*, 4639.
[6] C.-C. Lin, K. S. Anseth, *Pharm. Res.* **2008**, *26*, 631.
[7] N. A. Peppas, K. B. Keys, M. Torres-Lugo, A. M. Lowman, *J. Control. Release* **1999**, *62*, 81.
[8] N. A. Peppas, P. Bures, W. Leobandung, H. Ichikawa, *Eur. J. Pharm. Biopharm.* **2000**, *50*, 27.
[9] C. W. Tornoe, C. Christensen, M. Meldal, *J. Org. Chem.* **2002**, *67*, 3057.
[10] V. V. Rostovtsev, L. G. Green, V. V. Fokin, K. B. Sharpless, *Angew. Chem. Int. Edit.* **2002**, *41*, 2596.
[11] J. C. Jewett, C. R. Bertozzi, *Chem. Soc. Rev.* **2010**, *39*, 1272.
[12] J. A. Codelli, J. M. Baskin, N. J. Agard, C. R. Bertozzi, *J. Am. Chem. Soc.* **2008**, *130*, 11486.

[13] J. Dommerholt, S. Schmidt, R. Temming, L. J. A. Hendriks, F. P. J. T. Rutjes, J. C. M. van Hest, D. J. Lefeber, P. Friedl, F. L. van Delft, *Angew. Chem. Int. Ed.* **2010**, *49*, 9422.
[14] P. Thirumurugan, D. Matosiuk, K. Jozwiak, *Chem. Rev.* **2013**, *113*, 4905.
[15] A. B. Lowe, *Polym. Chem.* **2010**, *1*, 17.
[16] C. E. Hoyle, C. N. Bowman, *Angew. Chem. Int. Edit.* **2010**, *49*, 1540.
[17] A. A. Aimetti, A. J. Machen, K. S. Anseth, *Biomaterials* **2009**, *30*, 6048.
[18] H. Shih, C.-C. Lin, *Biomacromolecules* **2012**, *13*, 2003.
[19] N. K. Devaraj, R. Weissleder, S. A. Hilderbrand, *Bioconjugate Chem.* **2008**, *19*, 2297.
[20] D. L. Alge, M. A. Azagarsamy, D. F. Donohue, K. S. Anseth, *Biomacromolecules* **2013**, *14*, 949.
[21] H.-L. Wei, Z. Yang, L.-M. Zheng, Y.-M. Shen, *Polymer* **2009**, *50*, 2836.
[22] C. M. Nimmo, S. C. Owen, M. S. Shoichet, *Biomacromolecules* **2011**, *12*, 824.
[23] A. Borrmann, O. Fatunsin, J. Dommerholt, A. M. Jonker, D. W. P. M. Löwik, J. C. M. van Hest, F. L. van Delft, *Bioconjugate Chem.* **2015**, *26*, 257.
[24] A. M. Jonker, A. Borrmann, E. R. H. van Eck, F. L. van Delft, D. W. P. M. Löwik, J. C. M. van Hest, *Adv. Mater.* **2015**, *27*, 1235.
[25] O. Altintas, A. P. Vogt, C. Barner-Kowollik, U. Tunca, *Polym. Chem.* **2012**, *3*, 34.
[26] M. F. Debets, S. S. Van Berkel, J. Dommerholt, A. J. Dirks, F. Rutjes, F. L. Van Delft, *Accounts Chem. Res.* **2011**, *44*, 805.
[27] J. A. Burdick, K. S. Anseth, *Biomaterials* **2002**, *23*, 4315.
[28] E. Ruoslahti, *Annu. Rev. Cell Dev. Biol.* **1996**, *12*, 697.
[29] D. L. Hern, J. A. Hubbell, *J. Biomed. Mater. Res.* **1998**, *39*, 266.
[30] C. A. DeForest, B. D. Polizzotti, K. S. Anseth, *Nat. Mater.* **2009**, *8*, 659.
[31] J. Zheng, L. A. Smith Callahan, J. Hao, K. Guo, C. Wesdemiotis, R. A. Weiss, M. L. Becker, *ACS Macro Letters* **2012**, *1*, 1071.
[32] J. Xu, T. M. Filion, F. Prifti, J. Song, *Chem. -Asian J.* **2011**, *6*, 2730.
[33] D. Steinhilber, T. Rossow, S. Wedepohl, F. Paulus, S. Seiffert, R. Haag, *Angew. Chem. Int. Ed.* **2013**, *52*, 13538.
[34] D. E. Discher, *Science* **2005**, *310*, 1139.
[35] P. C. Georges, *J. Appl. Physiol.* **2005**, *98*, 1547.
[36] A. J. Engler, S. Sen, H. L. Sweeney, D. E. Discher, *Cell* **2006**, *126*, 677.
[37] T. Bai, F. Sun, L. Zhang, A. Sinclair, S. Liu, J.-R. Ella-Menye, Y. Zheng, S. Jiang, *Angew. Chem. Int. Ed.* **2014**, *53*, 12729.
[38] R. J. Pelham, Y. L. Wang, *Proc. Natl. Acad. Sci. U S A* **1997**, *94*, 13661.
[39] L. Richert, A. J. Engler, D. E. Discher, C. Picart, *Biomacromolecules* **2004**, *5*, 1908.
[40] V. E. G. Diederich, P. Studer, A. Kern, M. Lattuada, G. Storti, R. I. Sharma, J. G. Snedeker, M. Morbidelli, *Biotechnol. Bioeng.* **2013**, *110*, 1508.
[41] S. R. Peyton, C. B. Raub, V. P. Keschrumrus, A. J. Putnam, *Biomaterials* **2006**, *27*, 4881.
[42] C. M. Lo, H. B. Wang, M. Dembo, Y. L. Wang, *Biophys. J.* **2000**, *79*, 144.
[43] A. J. Engler, L. Richert, J. Y. Wong, C. Picart, D. E. Discher, *Surf. Sci.* **2004**, *570*, 142.
[44] A. Schneider, G. Francius, R. Obeid, P. Schwinte, J. Hemmerle, B. Frisch, P. Schaaf, J. C. Voegel, B. Senger, C. Picart, *Langmuir* **2006**, *22*, 1193.
[45] Z. Li, Y. Gong, S. Sun, Y. Du, D. Lü, X. Liu, M. Long, *Biomaterials* **2013**, *34*, 7616.
[46] B. Trappmann, J. E. Gautrot, J. T. Connelly, D. G. T. Strange, Y. Li, M. L. Oyen, M. A. C. Stuart, H. Boehm, B. J. Li, V. Vogel, J. P. Spatz, F. M. Watt, W. T. S. Huck, *Nat. Mater.* **2012**, *11*, 642.
[47] D. Missirlis, J. P. Spatz, *Biomacromolecules* **2014**, *15*, 195.
[48] J. P. Best, S. Javed, J. J. Richardson, K. L. Cho, M. M. J. Kamphuis, F. Caruso, *Soft Matter* **2013**, *9*, 4580.
[49] K. G. Robinson, T. Nie, A. D. Baldwin, E. C. Yang, K. L. Kiick, R. E. Akins, *J. Biomed. Mater. Res. A* **2012**, *100A*, 1356.
[50] I. Levental, P. C. Georges, P. A. Janmey, *Soft Matter* **2007**, *3*, 299.
[51] C. Yan, D. J. Pochan, *Chem. Soc. Rev.* **2010**, *39*, 3528.
[52] M. Arnold, E. A. Cavalcanti-Adam, R. Glass, J. Blümmel, W. Eck, M. Kantlehner, H. Kessler, J. P. Spatz, *ChemPhysChem* **2004**, *5*, 383.
[53] S. P. Massia, J. A. Hubbell, *J. Cell Biol.* **1991**, *114*, 1089.
[54] L. Y. Koo, D. J. Irvine, A. M. Mayes, D. A. Lauffenburger, L. G. Griffith, *J. Cell Sci.* **2002**, *115*, 1423.
[55] H. Tominaga, M. Ishiyama, F. Ohseto, K. Sasamoto, T. Hamamoto, K. Suzuki, M. Watanabe, *Anal. Commun.* **1999**, *36*, 47.
[56] H. Wang, L. Cai, A. Paul, A. Enejder, S. C. Heilshorn, *Biomacromolecules* **2014**, *15*, 3421.
[57] K. A. Kyburz, K. S. Anseth, *Acta Biomaterialia* **2013**, *9*, 6381.